

Mixed-time parallel evolution in multiple quantum NMR experiments: Sensitivity and resolution enhancement in heteronuclear NMR

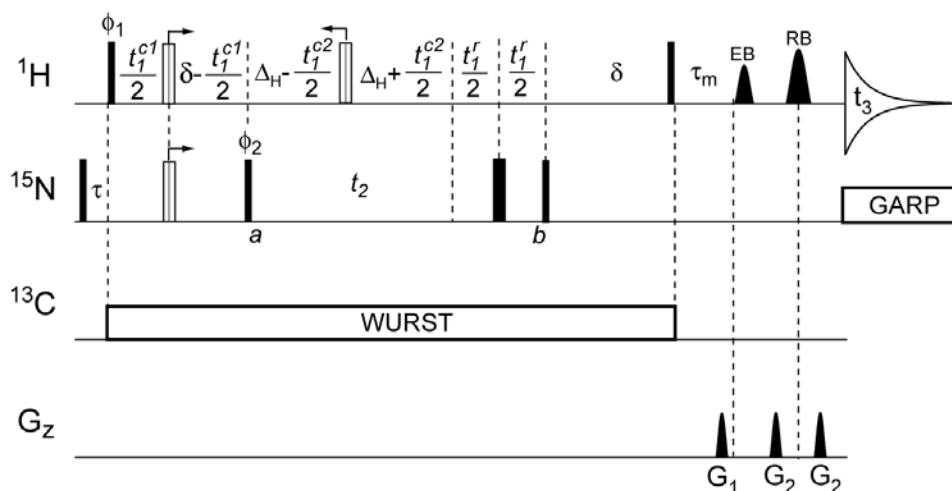
Jinfa Ying, Jordan H. Chill, John M. Louis & Ad Bax

Supplementary Material

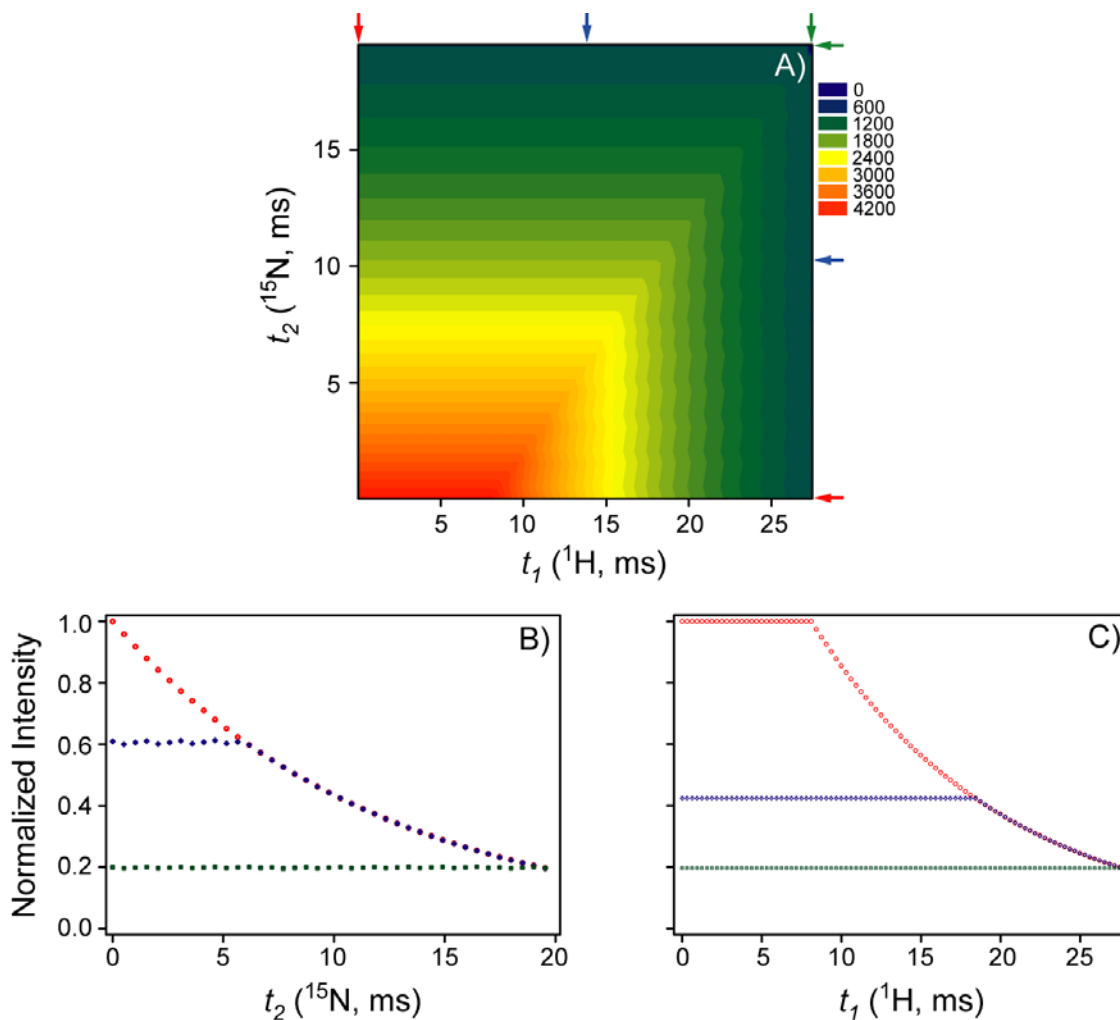
Figure 1 of the main text shows what the 3D MT-PARE-HMQC-NOESY pulse scheme actually “looks like” at different combinations of t_1 and t_2 values, and is conceptually simple. An equivalent scheme, that can be easier to code is shown in Supplementary Material Figure 1S. Actual pulse sequence code for both versions of the pulse program, written for a Bruker Avance system, can be downloaded from <http://spin.niddk.nih.gov/bax/pp/>.

In the scheme of Figure 1S, the delay t_2 for ^{15}N chemical shift evolution is always incremented in the outer loop of the pulse code, while the delay Δ_{H} is iteratively calculated at each t_2 point during the acquisition according to $\Delta_{\text{H}} = t_2/2$. In the inner loop of the pulse code (^1H dimension), the pair of 180° $^1\text{H}/^{15}\text{N}$ composite pulses is first moved toward time point a by incrementing the delay t_1^{c1} (equivalent to t_1 in Figure 1A, main text). Once the delay 2δ is fully exploited in the above constant-time manner, further ^1H constant-time evolution takes place by incrementing t_1^{c2} (equivalent to $t_1 - 2\delta$ in Figure 1B, main text), that is, by moving the composite 180° ^1H pulse during the PARE period toward time point a , until Δ_{H} cannot be further decremented. Finally, real-time t_1 evolution during t_1^{r} (equivalent to $t_1 - 2\delta$ in Figure 1C, main text) follows, if necessary, to fully record ^1H chemical shifts. An advantage of this approach in coding the sequence is that one delay (Δ_{H}) is kept in the inner loop, completely dependent on the other delay (t_2) in the outer loop. Note that, although t_2 is incremented linearly, constant-time evolution in t_2 still occurs due to the way this delay is also used for t_1 evolution, in parallel (see Figure 1C, main text and Supplementary Material Figure 2S).

Representative 1D slices of the simulated PARE data taken at the t_1 (or t_2) points indicated by colored arrows are shown in B) for the ^{15}N dimension and in C) for the ^1H dimension in corresponding colors. Note that a weak “ripple”, *i.e.* a periodic intensity fluctuation, is seen during the CT evolution (*i.e.* when $t_2 < t_1 - 2\delta$) in the t_2 (^{15}N) dimension, which is absent in the MT-PARE data when recored using the scheme of Figure 1 in the main text (see Figure 3, main text). The ripple results from the fact that incrementation in the t_2 dimension (dwell time $514 \mu\text{s}$ in our experiment and simulation) can be utilized for constant-time t_1 (dwell time $312 \mu\text{s}$) evolution, leaving a remainder of residual time during which relaxation but no chemical shift evolution occurs, and whose exact duration depends on the ratio of the two dwell times. The ripple effect disappears when the dwell times for the two PARE dimensions are chosen to be identical in the two dimensions. In practice, however, the intensity fluctuations fall far below the signal-to-noise and have vanishing effect on the final spectrum, and no limitations need be placed on dwell time selection when the scheme of Figure 1S is used.



Supplementary Material Figure 1S. Alternative version of the 3D MT-PARE-HMQC-NOESY pulse schemes presented in Figure 1 of the main text. Narrow and wide filled bars correspond to 90° and 180° pulses, respectively. Vertically hatched open bars represent composite pulses ($90^\circ_x 200^\circ_y 90^\circ_x$ for ^1H and $90^\circ_x 220^\circ_y 90^\circ_x$ for ^{15}N) employed to reduce RF inhomogeneity and off-resonance effects. Unless otherwise indicated, all pulses have phase x . The constant-time and real-time evolution in MT-PARE is differentiated by the superscripts c and r , respectively, of the incremented delays (i.e. t_1^r , t_1^{c1} , and t_1^{c2} etc.). The 90° $^1\text{H}^{\text{N}}$ shaped pulse (labeled as EB) with the EBURP-2 profile, (Geen and Freeman, 1991) has a duration of 1.2 ms (at 800 MHz ^1H frequency), and the pulse labeled as RB is 1.2-ms 180° $^1\text{H}^{\text{N}}$ shaped pulse with a REBURP profile. These pulses are centered at 8.28 ppm. Broadband ^{13}C decoupling was achieved using a sequence of adiabatic WURST pulses (Kupče and Freeman, 1995) with a sweep width of 28 kHz and ^{13}C WURST pulse durations of 10 ms (at 201 MHz ^{13}C frequency), centered at 117.5 ppm. Phase cycling: $\phi_1 = -x$; $\phi_2 = x, -x$; receiver = $x, -x$. Regular States-TPPI phase cycling of ϕ_1 and ϕ_2 was used to obtain quadrature detection in the ^1H (F_2) and ^{15}N (F_1) indirect dimensions, respectively. Delay durations: $\tau = 50$ ms; $\delta = 4.1$ ms; $\tau_m = 80$ ms; $\Delta_H = t_2/2$, i.e. iteratively calculated at each t_2 point during the acquisition. Pulsed field gradients are sine-bell shaped. The gradient pulses have durations of 2 ms and 1 ms, with peak amplitudes of 20 G/cm and 27 G/cm for G_1 and G_2 , respectively.



Supplementary Material Figure 2S. Intensity plot of the 2D time domain data simulated using the alternative MT-PARE pulse scheme shown in Supplementary Material Figure 1S. (B,C) Cross sections taken through the time domain data of (A) at the positions marked by the arrows in (A).